MIT Open Access Articles

Membrane-Based, Liquid–Liquid Separator with Integrated Pressure Control

Membrane-Based, Liquid-Liquid Separator with Integrated Pressure Control

Andrea Adamo,[†] Patrick L. Heider,[†] Nopphon Weeranoppanant, and Klavs F. Jensen*

Department of Chemical Engineering

Massachusetts Institute of Technology

77 Massachusetts Avenue

Cambridge, MA 02139, USA

ABSTRACT

We describe the development and application of an improved, membrane-based, liquid-liquid separator. Membrane based separation relies on the exploitation of surface forces and the use of a membrane wetted by one of the phases; however, successful separation requires accurate control of pressures making the operation and implementation cumbersome. Here we present an improved separator design that integrates a pressure control element to ensure that adequate operating conditions are always maintained. Additionally, the integrated pressure control decouples the separator from downstream unit operations. A detailed examination of the controlling physical equations shows how to design the device to allow operation across a wide range of conditions. Easy to implement, multistage separations such as solvent swaps and countercurrent extractions are demonstrated. The presented design significantly simplifies applications ranging from multistep synthesis to complex multistage separations.

INTRODUCTION

The last decade has seen a growing effort in the development of continuous flow chemical systems ranging from microscale[1-7] to milliscale.[8-13] The field has expanded in scope beyond single reactor and synthesis steps to multistep synthesis including intermediate workup and separation steps.[14-19] Among the separation techniques available to organic chemists, liquid-liquid separations are becoming more popular.[20] The small length scales encountered in continuous systems on the microscale and milliscale improve the extraction rate due to higher mass transfer coefficients,[21, 22] but present challenges for separation as surface forces dominate over the traditionally used gravity force.[23] Several solutions have reported including parallel

flow,[24-26] settling tanks,[27, 28] selectively wetting channels,[29-31] centrifugation,[13, 32] and microfiltration membranes.[19, 33] All of these separation techniques (except settling tanks and centrifugation) rely on the interfacial tension, γ, between the two liquids to provide the force to achieve separation.

Previous studies have demonstrated capillary pressure, P_{cap}, is a critical parameter which must be balanced with other forces in the device to guarantee proper operation of a separator.[19, 29, 33, 34] P_{cap} is given as

$$P_{cap} = \frac{2\gamma \cos(\theta)}{r} \tag{1}$$

where θ is the contact angle between the solid material of the device and two liquid phases and r is the radius of curvature of the interface. The design of each system is such that P_{cap} must be higher than the pressure difference across the interface, or separation will be incomplete. Since γ and θ are material properties that vary for each application, the only available design parameter is r which must be minimized to produce stable operation. In microscale systems, this is easy to do in a single channel with a small gap for parallel flow or two selectively wetting channels. Milliscale systems require larger channels to keep the pressure drop small relative to P_{cap} and therefore need many smaller channels to maintain high P_{cap} while permitting high flow rates. This is easily achieved using microfiltration membranes.[19, 33] Membrane-based separators are therefore ideal candidates for operating at both microscale[16] and milliscale.[19]

Previous analyses of membrane-based separators have focused on the importance of balancing the flow resistances through each outlet[33] or pressure control of individual outlets.[19, 29] These design criteria produce functioning devices; however, they make integration into larger systems difficult as downstream fluctuations can easily disrupt separation. A solution to this problem has been the use of break tanks and additional pumps[16] which increases the volume and complexity

of the systems. Break tanks with additional pumps can be eliminated by careful design for specific operating conditions at the cost of flexibility and robustness. Direct control of the pressure at the separator outlets can also avoid break tanks,[19] but still requires a feedback loop to account for differences in operating conditions downstream.

This paper reexamines the governing equations for separation in a membrane-based separator and presents a new separator design with an integrated pressure control component. The new design decouples the unit from downstream operations, increases flexibility, and eliminates the necessity for feedback control. Easy to implement solvent swap and countercurrent extraction examples are presented.

DESIGN THEORY

There are two main failure modes for membrane-based separators (Figure 1). The first is breakthrough of the retained phase which occurs when the pressure difference across the membrane (transmembrane pressure, ΔP_{mem}) is greater than P_{cap} (Figure 1b). The second failure mode is when the permeate phase is partially retained by the membrane and exits with the retained phase (Figure 1c). This occurs when there is insufficient pressure to cause the permeate liquid to flow through the membrane (P_{per}) which can be approximated by

$$P_{per} = \frac{8\mu QL}{n\pi R^4} \tag{2}$$

where μ is the viscosity of the permeate phase, Q is the entering permeate liquid volumetric flow rate, L is the membrane thickness, n is the number of pores and R is the pore radius. This assumes that the membrane acts as an array of cylindrical pores which is acceptable for this analysis as shown below. The value of P_{per} is the minimum pressure required to drive all of the permeate phase through the membrane using the entire area. Separation will still occur at values

of ΔP_{mem} greater than P_{per}, but the entire membrane area is not utilized (n is smaller such that Equation (2) equals ΔP_{mem}). In this case, the non-active pores support the additional pressure using the interfacial tension force. This is possible for values of ΔP_{mem} up to the point when breakthrough occurs, described as the first failure mode. A third failure mode exists where two phase streams exit both outlets, but this is indicative of operating the separator at a flow rate excessive for the available membrane area and therefore this condition is generally not encountered.

When the pressure drop along the length of the membrane channel is negligible compared to $P_{cap} - P_{per}$, then these two failure modes can be described in a single compound inequality

$$P_{cap} > \Delta P_{mem} > P_{per} \tag{3}$$

since ΔP_{mem} can be assumed to be constant along the membrane. This assumption is satisfied when the channel is sized so that pressure drops along its length are negligible. The first inequality is satisfied by appropriate selection of the membrane (material and pore size) while the second is better understood by replacing ΔP_{mem} with $P_1 - P_2$ where P_1 is the pressure on the retentate side of the membrane and P_2 is the pressure on the permeate side of the membrane and rewriting as

$$P_{cap} + P_2 > P_1 > P_{per} + P_2 \tag{4}$$

Equation (4) means that successful designs must always operate under conditions where the retentate pressure is some value greater than the sum of the permeate pressure and the P_{per} value for the maximum flow rate desired through the membrane.

Figure 1 shows a schematic of the membrane separator which incorporates a pressure control segment immediately following the membrane. The pressure control is made up of a diaphragm stretched over the retentate stream with the permeate stream flowing on the reverse side. Since

the diaphragm seals against the retentate flow path, no flow exits the retentate side of the separator unless $P_1 > P_2$. Additionally, the membrane is slightly deformed conveying an additional force on the retentate flow path that must be exceeded to permit flow. The differential pressure applied increases with the amount of deformation, the thickness of the diaphragm, and the elastic modulus of the diaphragm. This device then acts as a differential pressure controller such that $P_1 = P_{dia} + P_2$ where P_{dia} is the additional pressure due to the tension on the diaphragm. This simplifies Equation (4) to

$$P_{cap} > P_{dia} > P_{per} \tag{5}$$

which means that an appropriately designed separator will achieve complete separation as long as the flow rate through the membrane remains below maximum value for the design (that is pressure drops along channels are negligible).


EXPERIMENTAL SECTION

Figure 2 shows a photograph of a separator constructed out of polycarbonate. Better chemical compatibility was provided by constructing the separator out of high molecular weight polyethylene (HDPE). HDPE was selected because it was compatible with the solvents tested and did not deform or degrade. Even higher chemical compatibility could be provided by using materials such as ethylene tetrafluoroethylene (ETFE). The parts in the device were constructed using conventional machining tools and assembled with off the shelf screws and O-rings. The membranes used were Pall Zefluor 1 μm PTFE microfiltration membranes which are wet by the permeating organic phase and retain the aqueous phase with a total area of 280 mm^2 (roughly 35 mm long by 8 mm wide by 1 mm high). A PTFE membrane was selected because of its high chemical compatibility. No change in membrane performance was observed with different
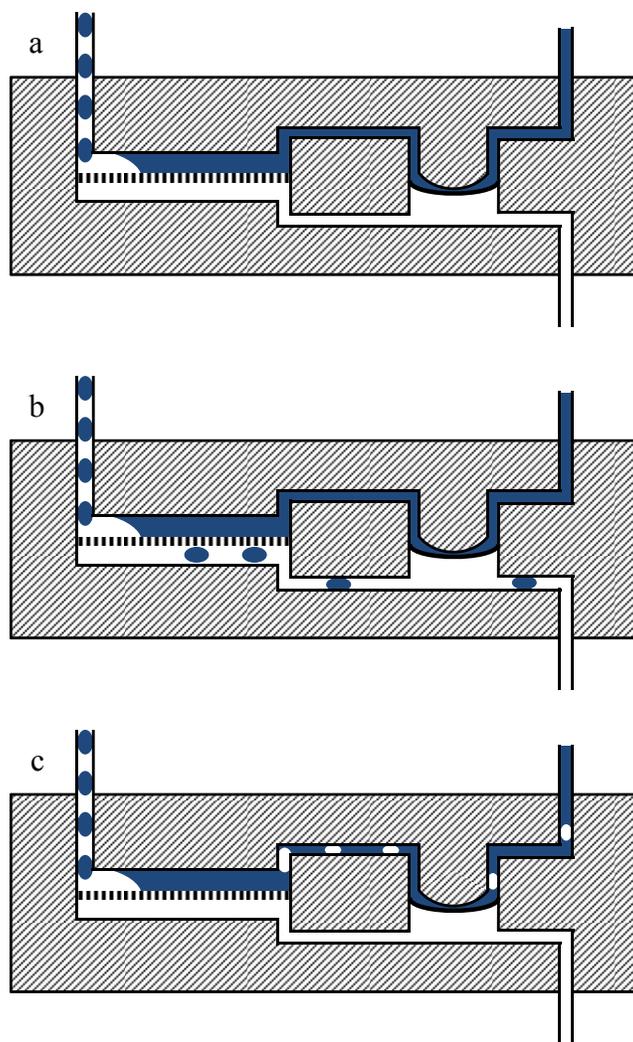
Figure 1. Integrated pressure control in membrane separator showing deformed diaphragm (heavy curved line) to provide a fixed pressure difference across the membrane (short vertical lines). The aqueous and organic phases are shown in blue and white respectively. (a) Separator under normal operation. (b) Separator operating with breakthrough of the retained phase. (c) Separator operating with retention of the permeate phase.

solvents due to mechanical changes in the membrane. The diaphragm was made of perfluoroalkoxy (PFA) film with a thickness of 25 μm and 50 μm. The 25 μm film provided a smaller pressure difference, but was prone to damage so the thicker film was used which was

more robust but provided a higher pressure difference (Figure 7). PFA was the only material tested for the diaphragm because it provides high chemical compatibility across a range of compounds commonly encountered in organic synthesis while other materials (such as various rubbers and elastomers) are susceptible to degradation in the presence of certain chemicals. All pumping was performed using piston pumps from Knauer (Smartline pump 100), Eldex (Optos 2SIP), and Fuji Techno Industries (Super metering pump HYM-08).
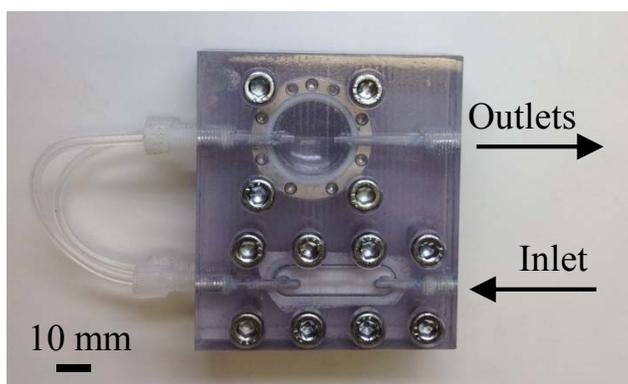

Figure 2. Photograph of polycarbonate membrane separator with integrated pressure control. The separator membrane is located on the lower portion and the pressure control diaphragm is located on the upper portion of the device.

The design equations were tested by removing the loops connecting the separation membrane with the differential pressure controller and attaching 235 cm of 1.6 mm inner diameter (ID) tubing to the permeate outlet and 60 cm of 0.76 mm ID tubing and 183 cm of 1.6 mm ID tubing to the retentate outlet. Previously contacted and separated water and ethyl acetate were each pumped at 5 mL/min into a tee mixer and then passed into the membrane separator. Pressure variations across the membrane were controlled by varying the height of the outlets over 2 m and calculating the pressure at the membrane. Failure points were calculated using Equation (3). The

values for R and L were taken from the manufacturer's specifications and n was calculated by measuring the membrane flow resistance by flowing only toluene and measuring the flow rate split between the two outlets. The value of γ was taken from the literature[35] as 36.1 mN/m for toluene-water and 6.8 mN/m for ethyl acetate-water. The differential pressure controller was tested by measuring the flow rate split between the two outlets when flowing only toluene through the device. 50 cm of 0.51 mm ID tubing was added to increase the pressure drop on the permeate side of the membrane so that flow exits both outlets.

Characterization of the new separator design where the membrane is coupled to the pressure controller was done following the set up represented in Figure 3. Hexane-water and ethyl acetate-water pairs were tested. The first one provided an initial test bed for the system with a wide operating range due to a high interfacial tension (50 mN/m), the second was a more challenging separation as the interfacial tension between the two fluids is an order of magnitude lower (6.8 mN/m) thus restricting the pressure difference operating window for successful separation. Flow rates between 2 and 8 mL/min for both the aqueous and organic phase were tested with these solvents as shown in Figure 3. Additionally to test the robustness of the pressure controller, the pressure in the collection reservoir of the organic side was changed to apply backpressure to the separator simulating downstream pressure drop (0, 1, 1.4, and 2 bar were used).
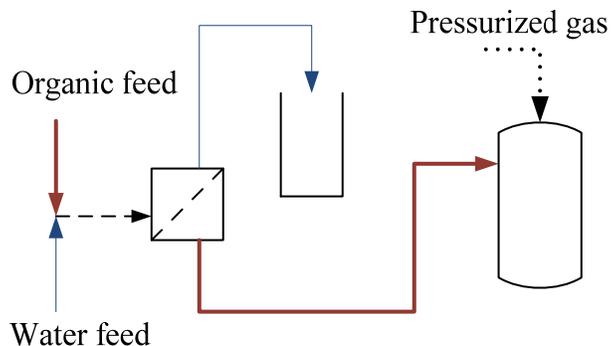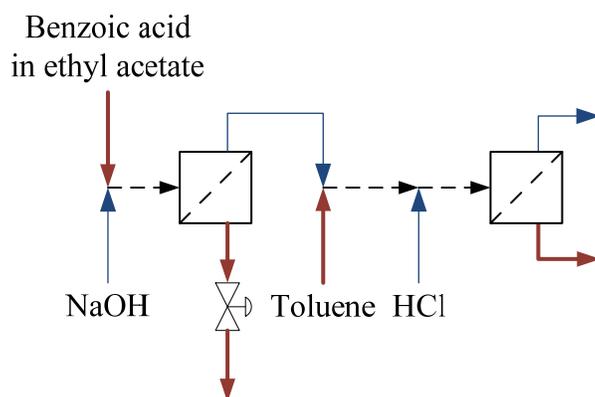
Figure 3. Setup for testing of membrane separator with integrated pressure control. Organic phase lines are shown in dark red, water lines are shown in blue, and two phase streams are shown as dashed lines. The organic outlet of the separator entered a closed vessel pressurized by a gas.

Solvent swap

A two stage solvent swap was tested as shown in Figure 4. A stream of 0.34 M benzoic acid in ethyl acetate was pumped at 1 mL/min into a mixing tee to contact a stream of 0.55 M NaOH flowing at 1 mL/min. A HDPE separator then split the phases with the organic phase passing through the membrane and through an additional 0.6 bar backpressure controller. This was added because the organic outlet of the separator generally must be at a higher pressure than the aqueous or else excess pressure on the aqueous outlet (in this case due to the second separator) will cause breakthrough of the aqueous phase by overriding the differential pressure controller. The aqueous phase containing benzoic acid then contacted a 1 mL/min stream of toluene. After a short length of tubing, a 1 mL/min stream of 0.6 M HCl was added. The stream was then separated by a second, identical membrane separator. Tubing with lengths to provide > 10 s of residence time was used to allow the streams to reach equilibrium prior to separation. All tubing used was 1.6 mm ID. The flow rate of each outlet stream was measured by collection in graduated cylinders and the concentration of benzoic acid determined by HPLC (Agilent 1100

with UV detector, 30 mM H_3PO_4 aqueous mobile phase, and 1:1 acetonitrile:methanol organic mobile phase). The results were compared to a comparable batch extraction performed at a 50 mL scale in separatory funnels with careful measurement of volumes.

Figure 4. Flow diagram of solvent swap setup. Organic phase lines are shown in dark red, water lines are shown in blue, and two phase streams are shown as dashed lines.

Countercurrent extraction

A three stage countercurrent extractor was set up as shown in Figure 5. Toluene and water were used as solvents with acetone as the extractant added at a 0.05 mass ratio to either solvent. The toluene feed was pumped by a single pump while a separate aqueous phase pump was used at each stage to increase the pressure so countercurrent operation was possible. All pumps were set to 3 mL/min. All tubing was 0.76 mm ID PFA with sufficient lengths to allow equilibrium before separation at each stage (residence time > 5 s). The outlet flow rates were measured and the concentration of acetone was determined by HPLC (Agilent 1100 with RI detector and 5 mM H_2SO_4 isocratic mobile phase) for the aqueous phase and GC (HP 6890 with FID detection) for the organic phase. Samples were taken after 15 min of operation with 3-5 repeats over the first hour. Performance was determined using standard countercurrent extraction plots.[36]
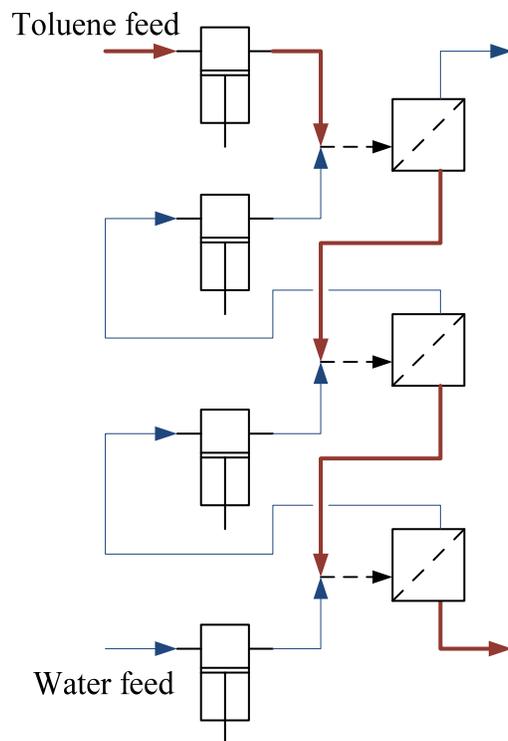
Figure 5. Flow diagram of countercurrent extraction setup. Organic phase lines are shown in dark red, water lines are shown in blue, and two phase streams are shown as dashed lines.

RESULTS AND DISCUSSION

The initial design of the separator was tested to confirm the assumptions from the theory section above held for the separator. The separator was operated without the differential pressure controller at 5 mL/min with a 1:1 ethyl acetate-water system. The results shown in Figure 6 compare the model predictions of the flow rate out the permeate side of the membrane with experimental results for varying ΔP_{mem}. While the performance of the separator is qualitatively similar to the model, breakthrough of the aqueous phase happens at much lower ΔP_{mem} values. This is indicative of a pore size distribution where a small number of pores with larger radii allow the aqueous phase through while the other pores still prohibit flow. This result is similar to

a bubble point test. A bubble point test, however, typically only identifies a critical pressure, converted to pore size using Equation (1), while this result shows a gradual increase in permeation as ΔP_{mem} is increased. This demonstrates that even if the largest pores are compromised, complete loss of separation will not occur as the low number of large pores cannot support the full flow of the retained phase. While Equation (5) can be expressed in terms of pore size distribution, separation should occur as long as the P_{cap} for the largest pores (determined empirically) is heeded. The large flat region in Figure 6 shows that the design parameters described above can be used to select an appropriate P_{dia} for the differential pressure controller to allow separation by operating below the empirically determined P_{cap}. Figure 7 shows that the differential pressure controller performance across a wide range of flow rates is fairly constant and within an acceptable range for most applications. The values of P_{cap} for both the toluene/water and ethyl acetate/water systems and the values of P_{per} for each flow rate bound the values for P_{dia} meaning the separator satisfies Equation (5) and should separate effectively. Figure 7 shows that even with increasing flow rate, P_{dia}, which equals ΔP_{mem} in the device, will remain constant and therefore separation performance remains constant. This is not true when the differential pressure controller is not present and downstream pressure drops change due to varying flow rates.
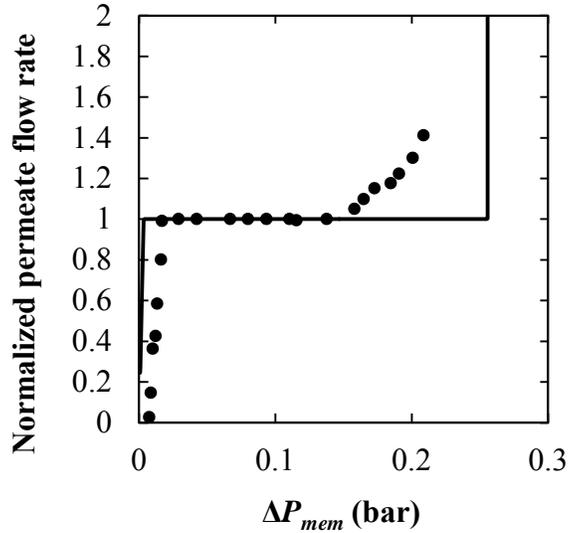
Figure 6. Plot of model and experimental results of the membrane separator without the pressure control diaphragm. The flow rate through the permeate outlet normalized by the inlet organic flow rate is plotted versus ΔP_{mem} where a value of 1 means perfect separation. Model values are given by the solid line while experimental values are given by circles. A flow rate of 5 mL/min for both water and ethyl acetate was used.
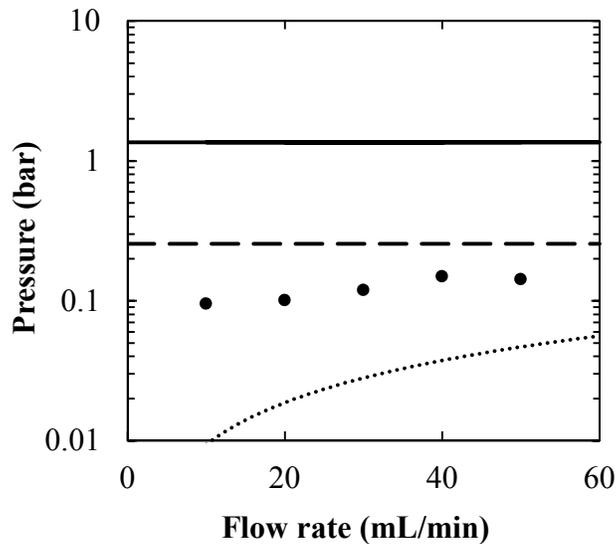
Figure 7. Plot of the differential pressure controller's performance, P_{dia}, versus flow rates (circles). The solid and dashed lines represent P_{cap} for a toluene-water and ethyl acetate-water separation respectively. The dotted line represents P_{per} for each flow rate. The separator meets the criteria of Equation (5) for all flow rates.

14

Results from the testing of the operation of a single separator with the integrated pressure controller are shown in Table 1. The table shows that as back pressure increases, a modest breakthrough can be observed for the ethyl acetate-water pair. This can be interpreted in light of the results of Figures 6 and 7. Figure 6 shows that the ethyl acetate-water system begins to allow breakthrough of the aqueous phase at 0.15 bar while Figure 7 shows that P_{dia} was between 0.1 and 0.15 bar for single phase flow. High pressures applied to the organic outlet cause small deviations in the performance of the pressure control diaphragm, slightly increasing P_{dia} which was sufficient to cause some breakthrough in the ethyl acetate-water system. Importantly, the hexane-water system has a sufficiently high P_{cap} that the small increase in did not cause any failure in separation across all the conditions tested.

Table 1. Summary of performance of a membrane separator with integrated pressure control

	Aqueous flow rate	Organic flow rate	Normalized permeate flow rate[a] Backpressure on organic outlet			
	mL/min	mL/min	0 bar	1 bar	1.4 bar	2 bar
Hexane-water	2	2	1	1	1	1
	5	5	1	1	1	1
	8	8	1	1	1	1
	2	8	1	1	1	1
	8	2	1	1	1	1
Ethyl acetate-water	2	2	1	1	1.0425	1.0500
	5	5	1	1.0108	1.0384	1.0930
	8	8	1	1.0159	1.0476	1.1180
	2	8	1	1	1.0625	1.2420
	8	2	1	1.0213	1.0492	1.0123

[a]The flow rate through the permeate outlet is normalized by the inlet organic flow rate (where 1 is perfect separation).

Solvent swap

The ability to change solvents between successive synthesis steps ('solvent swap') is an important consideration in using optimum solvent choices for the individual reactions. As a demonstration case, the separator was tested in a two stage solvent swap of benzoic acid from ethyl acetate to toluene. The results of the extraction are summarized in Table 2. The continuous system reproduces the batch performance both in terms of yield and mass balance. The system was operated for 2 h (corresponding to over 60 residence volumes) without any failure in the separation and halted without failure of the separation. No additional control was required beyond starting each pump up sequentially (the first stage pumps, then the second stage pumps). This application demonstrated how the separator effectively decouples the membrane pressures from effects downstream when the pressure on the organic outlet is greater than the aqueous outlet. The 0.6 bar of backpressure on the first stage permeate (organic) outlet would normally prevent flow without the presence of the differential pressure controller. Without the differential pressure control diaphragm, the backpressure would prevent all flow through the membrane and halt any separation. This is similar to the effect when a separator is used to separate an organic phase which contains the reactant for a subsequent reaction. Normally increased pressure required for a second reactor (to increase the boiling point of a solvent or due to a fixed bed) would require additional pressure control on the retentate (aqueous) side to closely match the organic pressure. The differential pressure controller simplifies the system by negating the need for the retentate side pressure control.

Table 2. Summary of solvent swap results comparing a batch shake flask and continuous with two membrane separators

	Yield[a]	Mass balance[a]
Continuous	0.92 +/- 0.006	0.97 +/- 0.008
Shake flask	0.94	0.96

[a]Error values are one standard deviation of 4 samples taken over the 2 h run.

A similar situation existed on the retentate side of the first separator in that it fed a second separator with a differential pressure controller that elevated the pressure. The effects of this pressure on the first separator were eliminated by adding a static backpressure regulator to the permeate side of the first separator larger than the highest pressure the retentate side might see. If this was not done, the first separator will not separate at all, but after adding the fixed regulator no additional control was required as long as the retentate pressure remained below 0.6 bar. The first stage was completely isolated from the second stage such that even during startup when the second stage was not running, the first stage will separate both streams. No additional adjustments were needed to maintain separation when the second stage was started up.

Countercurrent extraction

The separators were also tested in a countercurrent extraction setup. This required setting up one pump for the organic phase and a pump for the aqueous phase for each stage to drive the countercurrent flow. The separator achieved three stages of extraction (Figure 8) when extracting acetone from either toluene or water. This was expected since the high mass transfer rates in slug flow[21, 22] ensured that equilibrium was achieved before separation at each stage. Since extraction and separation occur independently, this system could be scaled to a large number of stages with
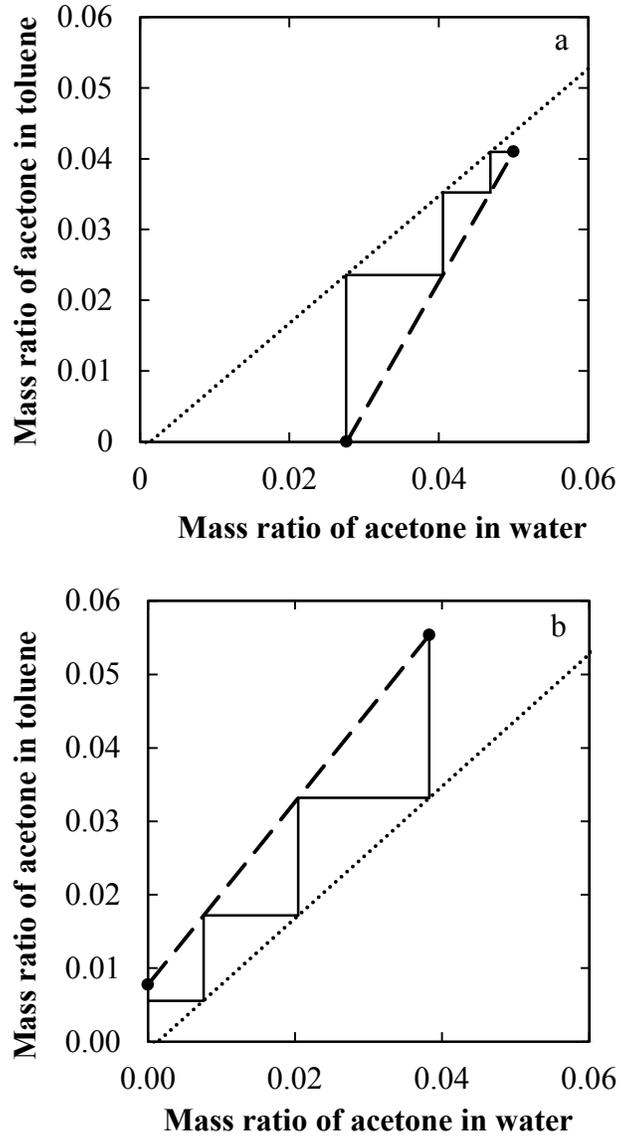
Figure 8. Extraction diagram for (a) extraction of acetone from water into toluene and (b) extraction of acetone from toluene into water. The equilibrium curve is shown by a dotted line and the operating line is shown by the dashed line; stages are stepped off with a solid line.

additional separators and pumps without any extraction efficiency issues. This is an improvement over other small scale countercurrent systems[24, 37, 38] which have a low number of stages and are limited in their flow rate by stage efficiencies related to the throughput. The

decoupling of the pressure in each stage makes the setup and operation of the countercurrent separator simple. The system needed to be initially primed with solvent for each phase as the piston pumps used could not handle two phase streams. After turning on each pump, the system then operated without any outside control for over 1 h, eliminating level control between stages for mixer/settler systems.[27]

CONCLUSIONS

The membrane-based separator presented here is an advance in continuous flow separators at the milliscale. The integrated pressure controller greatly reduces the complexity when implementing separators within chemical reactor systems by decoupling the separator pressures and limiting the online control required for operation. It is the first demonstration of countercurrent multi-stage liquid-liquid extraction using membrane based separators. Further, it simplifies multistep chemical systems including reactions coupled to separation and other multistage separations such as cross flow extraction. Larger systems which incorporate dynamic control would benefit from the intrinsic pressure control since control actions which affect downstream pressures (flow rate fluctuations, composition changes, etc.) can be tolerated without redesigning the system or additional control on the separator. The separator is useful in research settings since little additional changes are required to switch the separator between different applications. The specific design is especially suited to flow rates between 1 and 10 mL/min. Lower flow rates are possible although the residence time increases so a smaller device may be more appropriate depending on the application. Higher flow rates were also achieved (up to 40 mL/min) for systems with higher interfacial tension, limited by the pressure drop in the membrane channel compared to Equation (2). Future work to scale the separator down to μL/min

flows and determine the upper limits for scale up to larger separators using this design are

ongoing as well as applications to more complex, multistep syntheses.

AUTHOR INFORMATION

Corresponding Author

* E-mail: kfjensen@mit.edu. Tel.: +1-617-253-4589. Fax: +1-617-258-8224.

Author Contributions

[†] These authors contributed equally.

Notes

The authors declare no competing financial interest.

REFERENCES

(1)   Webb, D.; Jamison, T. F., Continuous flow multi-step organic synthesis. *Chem. Sci.* **2010,** 1, (6), 675-680.

(2)   Jensen, K. F., Microreaction engineering -- is small better? *Chem. Eng. Sci.* **2001,** 56, (2), 293-303.

(3)   Wiles, C.; Watts, P., Recent advances in micro reaction technology. *Chem. Commun.* **2011,** 47, (23), 6512-6535.

(4)   Hartman, R. L.; McMullen, J. P.; Jensen, K. F., Deciding Whether To Go with the Flow: Evaluating the Merits of Flow Reactors for Synthesis. *Angew. Chem. Int. Ed.* **2011,** 50, (33), 7502-7519.

(5)   Pennemann, H.; Watts, P.; Haswell, S. J.; Hessel, V.; Löwe, H., Benchmarking of Microreactor Applications. *Org. Process Res. Dev.* **2004,** 8, (3), 422-439.

(6)   Kockmann, N.; Gottsponer, M.; Zimmermann, B.; Roberge, D. M., Enabling Continuous-Flow Chemistry in Microstructured Devices for Pharmaceutical and Fine-Chemical Production. *Chem. Eur. J.* **2008,** 14, (25), 7470-7477.

(7)   Wegner, J.; Ceylan, S.; Kirschning, A., Ten key issues in modern flow chemistry. *Chem. Commun.* **2011,** 47, (16), 4583-4592.

(8)   Battilocchio, C.; Baumann, M.; Baxendale, I. R.; Biava, M.; Kitching, M. O.; Ley, S. V.; Martin, R. E.; Ohnmacht, S. A.; Tappin, N. D. C., Scale-Up of Flow-Assisted Synthesis of C2-Symmetric Chiral PyBox Ligands. *Synthesis* **2012,** 2012, (04), 635-647.

(9)   McMullen, J. P.; Jensen, K. F., Rapid Determination of Reaction Kinetics with an Automated Microfluidic System. *Org. Process Res. Dev.* **2011,** 15, (2), 398-407.

(10)   Cervera-Padrell, A. E.; Nielsen, J. P.; Jønch Pedersen, M.; Müller Christensen, K.; Mortensen, A. R.; Skovby, T.; Dam-Johansen, K.; Kiil, S.; Gernaey, K. V., Monitoring and Control of a Continuous Grignard Reaction for the Synthesis of an Active Pharmaceutical Ingredient Intermediate Using Inline NIR spectroscopy. *Org. Process Res. Dev.* **2012,** 16, (5), 901-914.

(11)   Kockmann, N.; Gottsponer, M.; Roberge, D. M., Scale-up concept of single-channel microreactors from process development to industrial production. *Chem. Eng. J.* **2011,** 167, (2–3), 718-726.

(12)   Hessel, V.; Löb, P.; Löwe, H., Industrial Microreactor Process Development up to Production. In *Microreactors in Organic Synthesis and Catalysis*, Wiley-VCH Verlag GmbH & Co. KGaA: 2008; pp 211-275.

(13)   Schuur, B.; Hallett, A. J.; Winkelman, J. G. M.; de Vries, J. G.; Heeres, H. J., Scalable Enantioseparation of Amino Acid Derivatives Using Continuous Liquid−Liquid Extraction in a Cascade of Centrifugal Contactor Separators. *Org. Process Res. Dev.* **2009,** 13, (5), 911-914.

(14)   Smith, C. J.; Nikbin, N.; Ley, S. V.; Lange, H.; Baxendale, I. R., A fully automated, multistep flow synthesis of 5-amino-4-cyano-1,2,3-triazoles. *Org. Biomol. Chem.* **2011,** 9, (6), 1938-1947.

(15)   Bogdan, A. R.; Poe, S. L.; Kubis, D. C.; Broadwater, S. J.; McQuade, D. T., The Continuous-Flow Synthesis of Ibuprofen. *Angew. Chem. Int. Ed.* **2009,** 48, (45), 8547-8550.

(16)   Sahoo, H. R.; Kralj, J. G.; Jensen, K. F., Multistep Continuous-Flow Microchemical Synthesis Involving Multiple Reactions and Separations. *Angew. Chem. Int. Ed.* **2007,** 46, (30), 5704-5708.

(17)   Varas, A. C.; Noël, T.; Wang, Q.; Hessel, V., Copper(I)-Catalyzed Azide–Alkyne Cycloadditions in Microflow: Catalyst Activity, High-T Operation, and an Integrated Continuous Copper Scavenging Unit. *ChemSusChem* **2012,** 5, (9), 1703-1707.

(18)   Hartman, R. L.; Naber, J. R.; Buchwald, S. L.; Jensen, K. F., Multistep Microchemical Synthesis Enabled by Microfluidic Distillation. *Angew. Chem. Int. Ed.* **2010,** 49, (5), 899-903.

(19)   Cervera-Padrell, A. E.; Morthensen, S. T.; Lewandowski, D. J.; Skovby, T.; Kiil, S.; Gernaey, K. V., Continuous Hydrolysis and Liquid–Liquid Phase Separation of an Active Pharmaceutical Ingredient Intermediate Using a Miniscale Hydrophobic Membrane Separator. *Org. Process Res. Dev.* **2012,** 16, (5), 888-900.

(20)   Tzschucke, C. C.; Markert, C.; Bannwarth, W.; Roller, S.; Hebel, A.; Haag, R., Modern Separation Techniques for the Efficient Workup in Organic Synthesis. *Angew. Chem. Int. Ed.* **2002,** 41, (21), 3964-4000.

(21)   Kuhn, S.; Jensen, K. F., A pH-Sensitive Laser-Induced Fluorescence Technique To Monitor Mass Transfer in Multiphase Flows in Microfluidic Devices. *Ind. Eng. Chem. Res.* **2012,** 51, (26), 8999-9006.

(22)   Burns, J. R.; Ramshaw, C., The intensification of rapid reactions in multiphase systems using slug flow in capillaries. *Lab Chip* **2001,** 1, (1), 10-15.

(23)   Günther, A.; Jensen, K. F., Multiphase microfluidics: from flow characteristics to chemical and materials synthesis. *Lab Chip* **2006,** 6, (12), 1487-1503.

(24)   Aota, A.; Nonaka, M.; Hibara, A.; Kitamori, T., Countercurrent Laminar Microflow for Highly Efficient Solvent Extraction. *Angew. Chem. Int. Ed.* **2007,** 46, (6), 878-880.

(25)   Aota, A.; Mawatari, K.; Kitamori, T., Parallel multiphase microflows: fundamental physics, stabilization methods and applications. *Lab Chip* **2009,** 9, (17), 2470-2476.

(26)   Aota, A.; Mawatari, K.; Takahashi, S.; Matsumoto, T.; Kanda, K.; Anraku, R.; Hibara, A.; Tokeshi, M.; Kitamori, T., Phase separation of gas–liquid and liquid–liquid microflows in microchips. *Microchim. Acta* **2009,** 164, (3), 249-255.

(27)   Hu, D. X.; O'Brien, M.; Ley, S. V., Continuous Multiple Liquid–Liquid Separation: Diazotization of Amino Acids in Flow. *Org. Lett.* **2012,** 14, (16), 4246-4249.

(28)   O'Brien, M.; Koos, P.; Browne, D. L.; Ley, S. V., A prototype continuous-flow liquid-liquid extraction system using open-source technology. *Org. Biomol. Chem.* **2012,** 10, (35), 7031-7036.

(29)   Castell, O. K.; Allender, C. J.; Barrow, D. A., Liquid-liquid phase separation: characterisation of a novel device capable of separating particle carrying multiphase flows. *Lab Chip* **2009,** 9, (3), 388-396.

(30)   Kashid, M. N.; Harshe, Y. M.; Agar, D. W., Liquid−Liquid Slug Flow in a Capillary: An Alternative to Suspended Drop or Film Contactors. *Ind. Eng. Chem. Res.* **2007,** 46, (25), 8420-8430.

(31)   Peroni, D.; van Egmond, W.; Kok, W. T.; Janssen, H.-G., Advancing liquid/liquid extraction through a novel microfluidic device: Theory, instrumentation and applications in gas chromatography. *J. Chromatogr. A* **2012,** 1226, (0), 77-86.

(32)   Schuur, B.; Floure, J.; Hallett, A. J.; Winkelman, J. G. M.; deVries, J. G.; Heeres, H. J., Continuous Chiral Separation of Amino Acid Derivatives by Enantioselective Liquid−Liquid Extraction in Centrifugal Contactor Separators. *Org. Process Res. Dev.* **2008,** 12, (5), 950-955.

(33)   Kralj, J. G.; Sahoo, H. R.; Jensen, K. F., Integrated continuous microfluidic liquid-liquid extraction. *Lab Chip* **2007,** 7, (2), 256-263.

(34)   Hartman, R. L.; Sahoo, H. R.; Yen, B. C.; Jensen, K. F., Distillation in microchemical systems using capillary forces and segmented flow. *Lab Chip* **2009,** 9, (13), 1843-1849.

(35)   Donahue, D. J.; Bartell, F. E., The Boundary Tension at Water-Organic Liquid Interfaces. *J. Phys. Chem.* **1952,** 56, (4), 480-484.

(36)   Seader, J. D.; Henley, E. J., *Separation Process Principles*. 2nd ed.; John Wiley & Sons, Inc.: 2006.

(37)   Lam, K. F.; Cao, E.; Sorensen, E.; Gavriilidis, A., Development of multistage distillation in a microfluidic chip. *Lab Chip* **2011,** 11, (7), 1311-1317.

(38)   Zhang, Y.; Kato, S.; Anazawa, T., Vacuum membrane distillation by microchip with temperature gradient. *Lab Chip* **2010,** 10, (7), 899-908.

TABLE OF CONTENTS GRAPHIC